JOURNAL OF MATERIALS SCIENCE 19 (1984) 1799–1804

Annealing studies of cold-rolled Ni_3Al

I. BAKER, D. V. VIENS, E. M. SCHULSON
Thayer School of Engineering, Dartmouth College, Hanover, New Hampshire 03755, USA

Annealing studies of cold-rolled Ni_3Al established that the recrystallization kinetics obey the Avrami equation and that the grain-growth kinetics obey the relation $\bar{d} = Ct^n$ where $\bar{d}$ is the average grain size, t the time and C and n are parameters whose magnitude depends on temperature. Disorder is introduced during deformation but subsequently removed during recrystallization. Antiphase boundaries are found in some recrystallized grains but do not show any preference to lie on {1 0 0} planes, contrary to predictions based on Flinn's nearest-neighbour approximation model. Twins, dislocation networks an planar faults are also found in recrystallized grains.

1. Introduction

Aluminide intermetallics are strong, microstructurally stable and oxidation-resistant at elevated temperatures, and are, thus, potentially useful in advanced energy conversion systems. However, whilst they show ductility as single crystals in polycrystalline form they are generally brittle under ambient conditions. For this reason, they are not utilized as engineering materials. A way to improve the ductility of polycrystalline aluminides may be to produce grain sizes smaller than that at which the ductile to brittle transition occurs [1]. One route to grain refinement is through deformation and subsequent recrystallization.

This paper is concerned with recrystallization in Ni_3Al, an Ll_2 aluminide which is highly ordered up to melting at 1658 K [2]. Its purpose is to present the kinetics of recrystallization and grain growth and the microstructures developed during the processes.

2. Experimental details

A single crystal of nickel-rich Ni_3Al (23.9 ± 0.4 at% Al) was obtained from United Technologies, East Hartford, Connecticut, USA. The principal impurities (in at%) were silicon (0.050), chromium (0.029), copper (0.008), cobalt (0.025) and lead (< 0.002). The crystal was sectioned into strips 2.5 mm thick which had approximately {1 1 1} surfaces (6 mm x 25 mm) in the rolling plane and a ⟨1 1 0⟩ axis along the rolling direction.

The strips were cold-rolled in steps of about 10% reduction in area until edge-cracking occurred at a total reduction of 59 ± 4% (1 mm thick). Pieces were then annealed in dried and deoxygenated flowing argon for various times at temperatures from 973 to 1173 K, ± 5 K. Recrystallization was followed by optical examination of mounted and polished specimens etched in Marble's reagent and by microhardness measurements. In addition transmission electron microscope specimens were prepared from the samples annealed at 1061 K by electropolishing 3 mm discs to perforation in 10% sulphuric acid in methanol at 65 mA in a PTFE holder at 0° C.

3. Results and discussion

TEM foils were taken from rolling plane sections only. Thus, the microstructural detail which was seen in as-rolled samples was only a mat of dislocations showing a directionality consistent with a rolling deformation. Selected-area diffraction patterns (Fig. 1) indicated that some disordering had taken place during deformation, evident from the low relative intensities of superlattice reflections (compared with Fig. 7, described below). Disordering of Ni_3Al by deformation has been noted by others using X-ray diffraction [3–5], and, presumably indicates the creation of antiphase domain boundaries through the glide of $a/2$ ⟨1 1 0⟩ superlattice partial dislocations or the creation of complex stacking faults through the glide of $a/6$ ⟨2 1 1⟩ partials.

Fig. 2 shows the hardness of Ni_3Al as a func-

0022–2461/84 $03.00 + .12

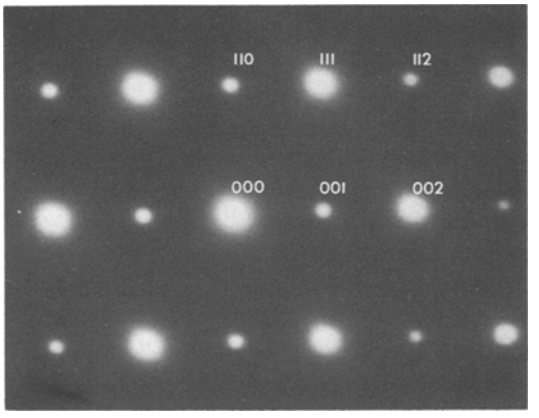

Figure 1 Selected-area diffraction pattern from an as-rolled specimen. Superlattice reflections are relatively weak, compared with those in Fig. 7.

tion of time at different annealing temperatures. A decrease in hardness occurs before the onset of recrystallization (as determined from optical micrographs) which is indicated on the curves, implying that a large amount of recovery precedes recystallization. Indeed, both optical micrographs and transmission electron micrographs of annealed, partially recrystallized, specimens reveal a recovered structure consisting of subgrains of about 5 μm average diameter (Fig. 3). It should also be noted that a few regions were found which did not have a subgrain structure but remained as elongated regions, although extensive recovery (i.e. dislocation rearrangement) had still occurred (Fig. 4).

Fig. 5 shows the recrystallization kinetics. The curves are of the familiar sigmoidal shape, typical of nucleation and growth, and may be expressed by the Avrami equation:

$$X_v = 1 - \exp(-Bt^k),$$

where X_v is the volume fraction recrystallized, t is time and B and k are experimentally determined parameters. Separate plots of ln [ln $(1/1 - X_v)$] against ln t revealed values of k between 1 and 2, suggesting one-dimensional growth. No consistent trend in k as a function of temperature was noted. The values of B mainly increase with temperature from 9.66×10^{-7} sec$^{-1.25}$ at 1008 K to 5.53×10^{-5} sec$^{-1.69}$ at 1173 K. This increase reflects an increase in either or both the nucleation and the growth rates as the temperature is raised.

Fig. 6 shows an Arrhenius plot of the reciprocal times for 0.5 fraction recrystallized; the slope yields an apparent activation energy of 331 kJ mol^{-1}. The fundamental significance of this activation energy is not clear because it embodies both nucleation and growth kinetics. However, noteworthy is its similarity to the value of 309 kJ mol^{-1}

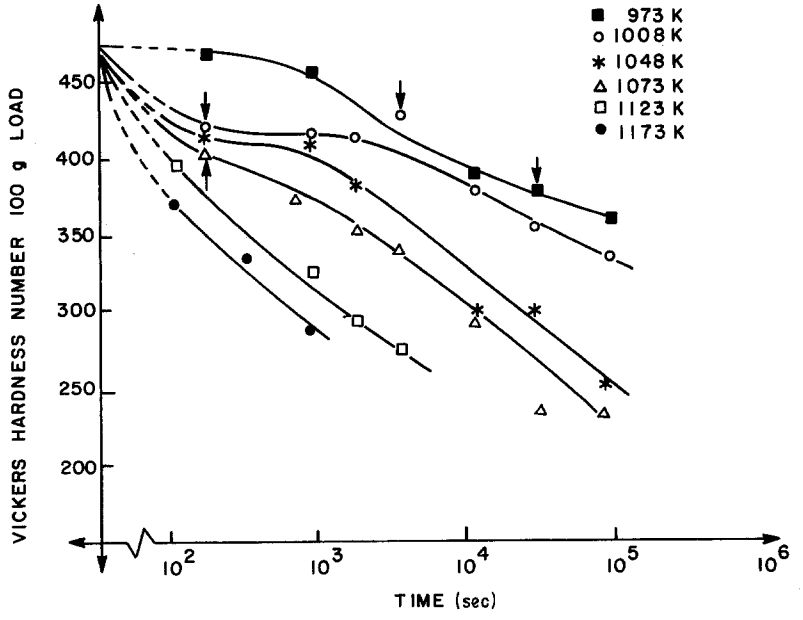

Figure 2 Graph showing the reduction of hardness of Ni_3Al with increasing time at various temperatures. Arrows indicate the point at which recrystallization was first detected optically. (Each point is the average of 15 measurements taken with 100 g load for 15 sec.)

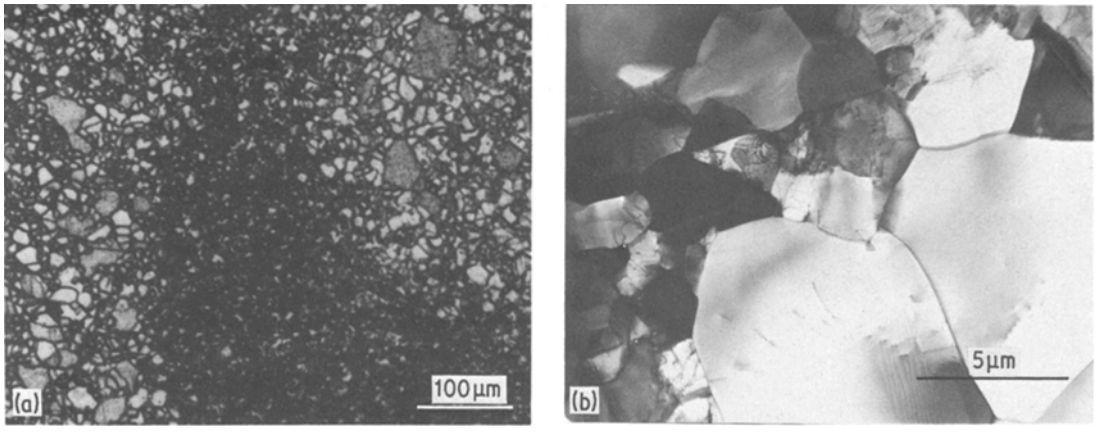

Figure 3 Rolled Ni_3Al annealed at 1061 K for: (a) 2580 sec, $X_v = 0.28$, optical micrograph showing an unrecrystallized area containing subgrains bounded by recrystallized regions, and (b) 1980 sec, $X_v = 0.16$, electron micrograph showing two recrystallized grains growing into the recovered structure comprised of subgrains.

for the activation energy for diffusion of nickel through Ni_3Al containing 23.8 at % aluminium [6]; i.e. of essentially the same composition as the alloy studied here. In another strongly ordered nickel aluminide, the B2 compound NiAl, the apparent activation energy for recrystallization also agrees favourably with the activation energy for the diffusion of nickel [7]. Thus, it appears that the diffusivity of nickel may be an important factor in the recrystallization of nickel aluminides.

The recrystallized material has several structural features worthy of note. Twin boundaries across grains and discrete twins are common. Fig. 7 shows a $(1\bar{1}0)$ matrix pattern with twin spots in positions corresponding to a matrix spot $\pm \frac{1}{3}[111]$ i.e. a [111] twin axis with the twin plane parallel to the beam. The relative intensity of the superlattice reflections is larger than in Fig. 1, indicating that the material is more fully ordered after recrystallization.

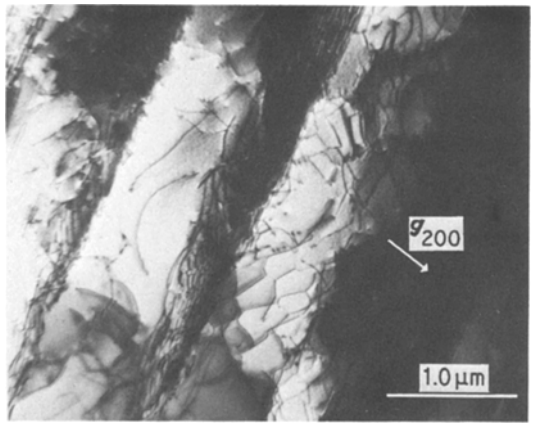

Figure 4 Rolled Ni_3Al annealed for 2880 sec at 1061 K, $X_v = 0.55$, bright-field electron micrograph showing one of the few areas which did not recover to a subgrain structure.

Antiphase boundaries are present in only a few recrystallized grains (Fig. 8) having $a/2\langle 110\rangle$ type displacement vectors. An interesting point is that they do not show a preference to lie on any specific plane. This point is reinforced by the loop of APB shown in Fig. 8b. Calculations of the APB energy in the Ll_2 structure by Flinn [8] based on a nearest-neighbour approximation first suggested that APBs, particularly thermally-induced ones, should lie on {100} planes. This concept, whilst originally supported by observations of thermally-induced APBs in Cu_3Au [9], is not, however, supported by observations of APBs in Ni_3Al either in this paper or in similar observations by Calvayrac and Fayard [10]. Thus the validity of the nearest-neighbour approximation for determining APB energies must be questioned as must some of the dislocation mechanisms based on cross-slip to and subsequent pinning on {100} planes proposed to explain the anomalous temperature dependence of some of the properties of Ni_3Al.

Other features are dislocation networks and planar faults (Fig. 9), similar in appearance to those found after deformation and annealing of the isostructural intermetallic Zr_3Al [11]. Whilst some planar faults are {111} stacking faults, others do not lie on {111} planes.

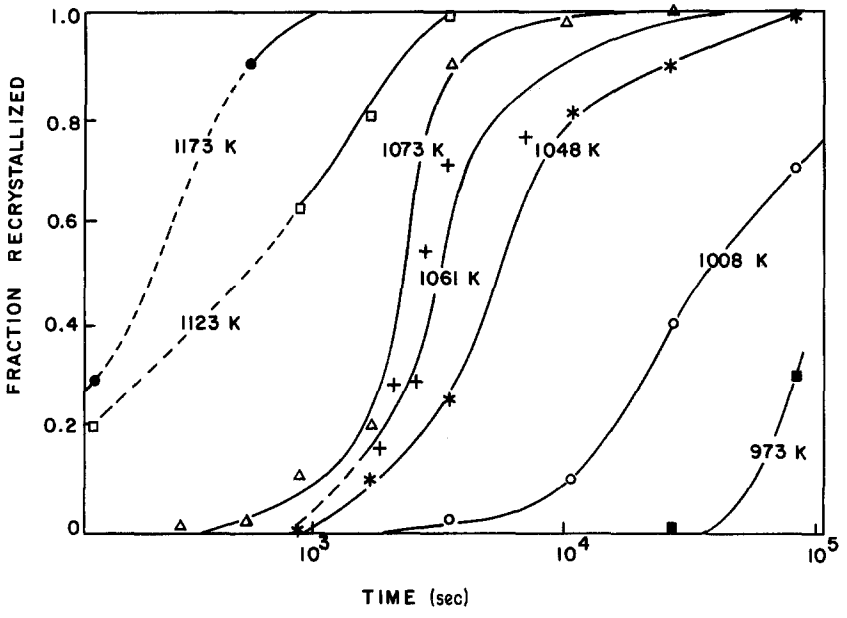

Figure 5 Isothermal transformation curves illustrating the recrystallization kinetics of Ni_3Al cold-rolled by 59%.

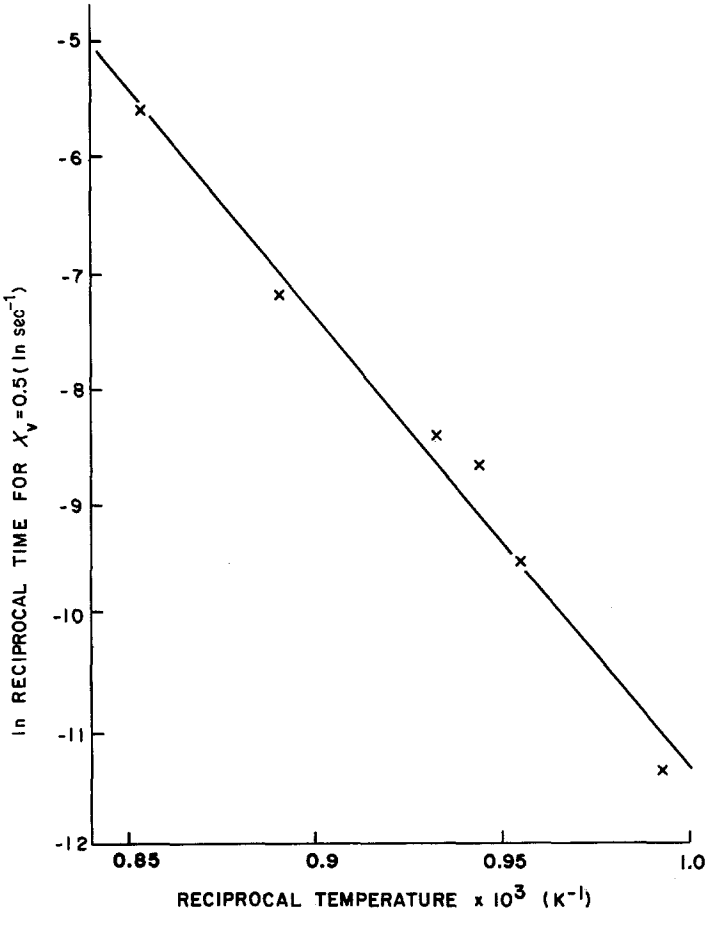

Figure 6 An Arrhenius plot of the reciprocal time for a fractional recrystallization of 0.5 for the data shown in Fig. 5. The slope yields an apparent activation energy of 331 kJ mol^{-1}.

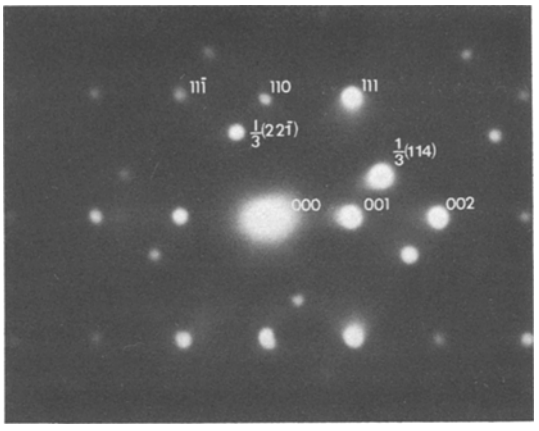

Figure 7 Selected-area diffraction pattern from grain shown in Fig. 8 containing a twin. The spots $\frac{1}{3}(22\bar{1})$ and $\frac{1}{3}(114)$ are due to twinning about a [111] twin axis. Note superlattice reflections (001) and (110) are relatively much stronger than those in the cold-rolled material, cf. Fig. 1.

The grain size resulting from primary recrystallization was 9 μm meaning that a large driving force is present for subsequent normal grain coarsening. At the three temperatures at which the grain growth kinetics were measured, they obeyed the relation:

$$\bar{d} = Ct^n$$

where $\bar{d}$ is the average instantaneous grain diameter*, t is time and C and n are materials constants (Fig. 10). The constant C includes a term for the mobility of a grain boundary, thus should increase with increasing temperature, as observed, i.e. ($C = 0.36\,\mu\text{m sec}^{-0.36}$ at 1073 K, $0.74\,\mu\text{m sec}^{-0.37}$ at 1173 K and $3.64\,\mu\text{m sec}^{-0.27}$ at 1273 K). The values of the exponent n (i.e. 0.36 at 1073 K, 0.37 at 1173 K, 0.27 at 1273 K deviated from the theoretical value of $n = 0.5$ (for a pure material) as is commonly found, implying an impediment to grain-boundary migration.

4. Conclusions

From observations on the structure of cold rolled (59% reduction in area) and annealed single crystals of Ni_3Al (23.9 at % aluminium) it is concluded that:

1. disorder occurred during cold-rolling whilst recrystallization restored order, confirming earlier X-ray work [3–5];

2. subgrains form and hardness drops prior to the onset of recrystallization, i.e. recovery occurs;

3. the recrystallization kinetics obey the Avrami equation. The apparent activation energy for recrystallization (331 kJ mol^{-1}) is similar to the activation energy for diffusion of nickel in Ni_3Al (309 kJ mol^{-1});

4. planar faults, dislocation networks, twins and APBs were present in some recrystallized grains. APBs did not show a preference to lie on {100} planes and even existed as loops;

5. grain growth kinetics obey the relation $\bar{d} = Ct^n$ where $\bar{d}$ is the average grain diameter, t is time and C and n are constants which depend on the annealing temperature.

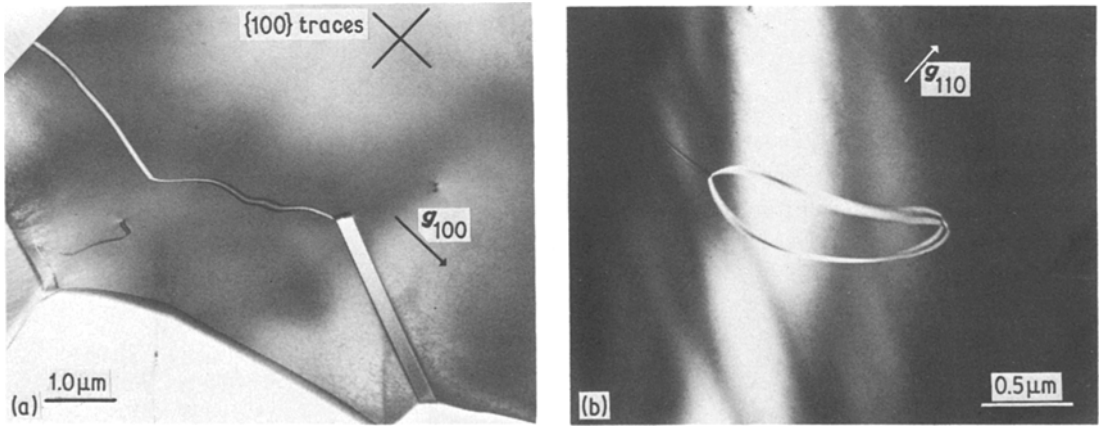

Figure 8 Electron micrograph of rolled Ni_3Al annealed for 1980 sec at 1061 K, $X_v = 0.16$: (a) bright-field image of APBs; the feature in the lower right is a twin. Note that the APB does not coincide with the {1 0 0} traces. (b) dark-field image of an APB loop.

*$\bar{d}$ is the average distance between grain boundaries as seen on metallurgical sections, measured using a linear intercept method.

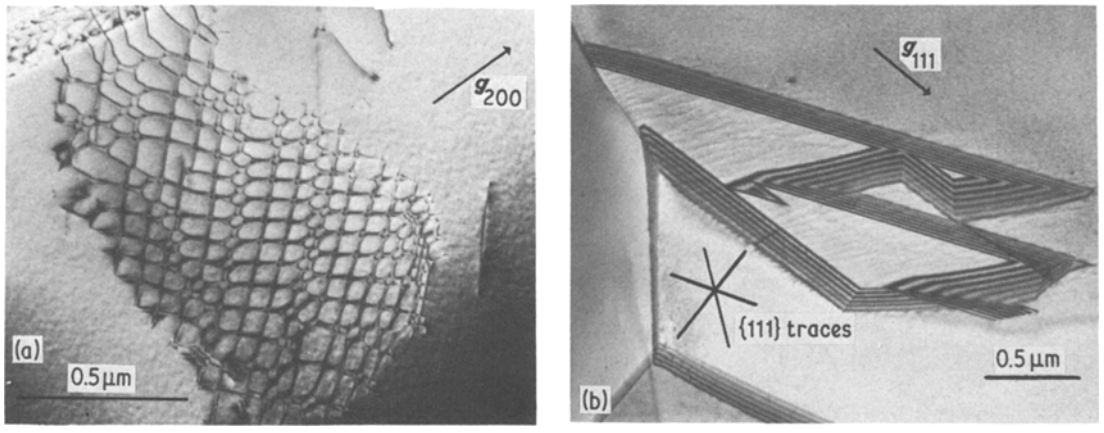

Figure 9 Electron micrograph of other features found in recrystallized grains: (a) bright-field image of dislocation network in Ni_3Al annealed for 3600 sec at 1061 K, $X_v = 0.70$; (b) bright-field image of planar faults present in Ni_3Al annealed for 1980 sec at 1061 K, $X_v = 0.16$. Note that not all faults have planes parallel to {1 1 1} traces.

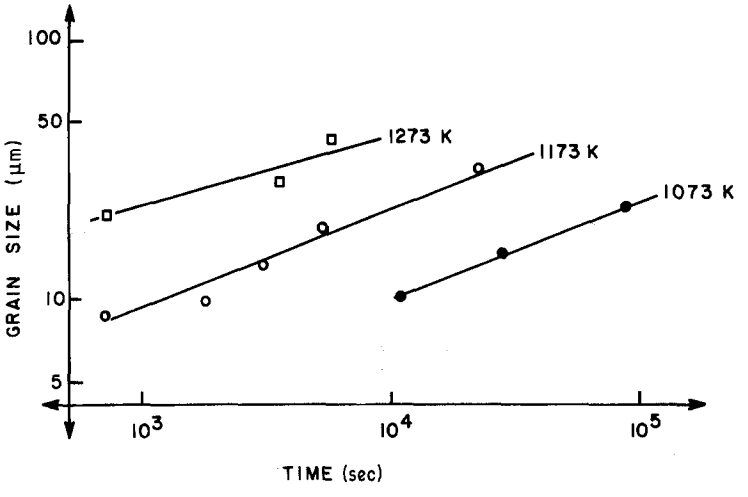

Figure 10 Grain-growth curves for Ni_3Al previously recrystallized to a grain size of 9 μm.

Acknowledgement

The work was supported by the Office of Basic Energy Sciences, US Department of Energy, Contract no. DE-AC02-81ER10907.

References

1. E. M. SCHULSON, *Res. Mech. Lett.* 1 (1981) 111.
2. SHWU-JIAN LIANG and D. P. POPE, *Met. Trans.* 7A (1976) 887.
3. C. L. COREY and D. I. POTTER, *J. Appl. Phys.* 38 (1967) 3894.
4. J. P. CLARK and G. P. MOHANTY, *Scripta. Metall.* 8 (1974) 959.
5. F. W. ARNOTH, J. P. CLARK and G. P. MOHANTY, *J. Appl. Phys.* 48 (1977) 1771.
6. G. F. HANCOCK, *Phys. Status Solidi* (*a*) 7 (1971) 535.
7. G. R. HAFF and E. M. SCHULSON, *Met. Trans. A* 13A (1982) 1563.
8. P. A. FLINN, *Trans. AIME* 218 (1960) 145.
9. M. J. MARCINKOWSKI, "Electron Microscopy and the Strength of Crystals", edited by G. Thomas and J. Washburn (Interscience, New York, 1963) p. 421.
10. Y. CALVAYRAC and M. FAYARD, *Acta Metall.* 14 (1966) 783.
11. L. M. HOWE, M. RAINVILLE and E. M. SCHULSON, *J. Nucl. Mater.* 50 (1974) 139.

Received 19 August
and accepted 13 September 1983